Quantification of Laminar Mixing Performance using Laser-Induced Fluorescence

Oliver Pust[1], Tyson Strand[2], Peter Mathys[3], Armin Rütti[4]

1: TSI GmbH, Aachen, Germany, oliver.pust@tsi.com
2: TSI Incorporated, Shoreview, USA, tyson.strand@tsi.com
3: Sulzer Chemtech Ltd, Winterthur, Switzerland, Peter.Mathys@sulzer.com
4: Sulzer Chemtech Ltd, Winterthur, Switzerland, Armin.Ruetti@sulzer.com

Abstract The following examines the application of planar laser-induced fluorescence (PLIF) to the assessment and quantification of mixing performance. Although important in a variety of industries and applications, evaluation of mixing performance has historically been challenging due, in part, to variations in measurement methods and evaluation criteria among different fields of study. The demonstrated ability of the PLIF technique to provide spatial concentration distributions of a contaminant or mixing species in a planar region within optically accessible gaseous and liquid flows makes it an increasingly common choice for mixing analysis investigations. PLIF measurements are presented of the concentration field in a cross-sectional area at the outlet of an SMX static mixer for laminar flows, for varying values of the (normalized) mixing length L/D. The measured concentration fields allow quantification of changes in the mixing performance via numerous statistical and geometric measures. In particular, the coefficient of variation (standard deviation divided by the mean concentration value) is used to measure of mixture homogeneity and evaluate the effect of changes in the mixing length. Profile graphs of concentration values are used to examine changes in the thickness of the fluid layers.

1. Introduction

From fundamental studies of turbulent transport processes to applications such as IC engine flows and microfluidics, evaluation and optimization of mixing performance is a common requirement in a range of industrial and academic settings. Consistency and uniformity among measurement campaigns across differing disciplines is generally not possible due, in part, to extensive variations in the type of mixing processes under investigation, the variety of measurement techniques used, and the unique measurement challenges posed by specific flow situations. Examples of measurement techniques that have been applied to mixing analysis include conductivity measurements, 'freezing' the transient fluid distribution and cutting away sections to quantify the concentration distribution, qualitative flow visualization, and various tomographic methods, as well as planar laser-induced fluorescence (PLIF). PLIF has become an increasingly common technique for assessing mixing performance in optically accessible gaseous and liquid flows due to the inherent non-intrusive nature of the measurement, as well as the high accuracy of the measured spatial concentration distribution. In some slower flows (or utilizing recent technological advances in camera frame rates and laser pulse repetition rates for faster flows) and for certain periodic flows, the PLIF technique can also be used to measure temporal changes in the concentration field (Crimaldi and Koseff 2001), permitting a more detailed analysis of mixing processes.

PLIF measurements of mixing appear across a range of disciplines (including combustion diagnostics, fundamental turbulence and fluid mechanics, microfluidics, environmental engineering, contaminant hydrogeology, and industrial mixing processes) for a range of different flow applications (such as turbulent flow analysis, laminar mixing, IC engine flows, micron scale flows, wake flows, and injector flows). Although the measurement goals vary according to the specific application, the measured parameters are all similar in that they act as indicators of the extent or

efficiency of a mixing process.

PLIF measurements can be performed in most optically accessible flows, and have thus been used to examine mixing processes in both liquid (e.g. Aguirre et al. 2006; Xi et al. 2004; and Hjertager et al., 2003) and gaseous (e.g. King et al. 1997; Probst et al. 2001; and Kaiser and Long 2004) phase flows. The choice of tracer species depends upon the flow situation and scalar field of interest (concentration, temperature) (King et al. 1997; Ritchie and Seitzman 2001; Tian and Roberts 2003; Kaiser and Long 2005).

The influence of noise and finite spatial resolution issues must be considered during PLIF experiments. Crimaldi and Koseff (2001) performed PLIF measurements of a contaminant (odorant) plume in a turbulent boundary layer, using Rhodamine 6G seeded effluent in water to make high spatial resolution measurements of the concentration structure in the plume, and summarizing the relationship between the spatial measurement resolution and the thickness of the laser light sheet. Other quantities calculated from the concentration field, such as scalar dissipation rates, mixing length scales, and molecular mixing rates are also affected (King et al. 1997; Tsurikoz and Clemens 2002; Ghandhi 2005).

2. Experimental Setup

PLIF measurements of concentration were performed at varying distances downstream of a commercial static mixing device (Sulzer SMX mixer, Figure 1). The mixer was positioned in a vertical pipe with fluids flowing upward through the device. Two unmixed fluid streams were introduced immediately below the static mixer. One fluid stream was a glucose solution seeded with Rhodamine 6G as a fluorescent tracer species, while the other stream was unseeded glucose solution. A tracer concentration of 50 µg/L was used. Separate measurements were performed to determine the binary diffusion coefficient between the unseeded fluid stream and the stream seeded with the Rhodamine 6G tracer, for comparison to CFD simulations of the mixing process. Rhodamine 6G was chosen as the tracer species due to the relatively high fluorescence yield, as well as the broad absorption feature with a peak near 525nm (near the readily available 532nm YAG harmonic) and emission feature with a peak near 560nm.

Fig. 1. Sulzer SMX mixers for the laminar flow regime

The experimental arrangement is shown in Figure 2. The 532nm output of a frequency doubled Nd:YAG was formed into a horizontal laser light sheet using a -25mm cylindrical lens, with a 500mm spherical lens to produce a narrow waist (thickness) of the sheet at the measurement region. The typical light sheet thickness at the measurement region was approximately 400 μm. The light sheet illuminated a horizontal cross section. Above the measurement region, the flow was diverted radially by a transparent plate. A peltier-cooled CCD camera (TSI PowerView 14-10) equipped with a 550nm long wave pass filter was oriented vertically, viewing downward at the region illuminated by the laser light sheet. All hardware timing, and image capture, processing, and display operations were performed with the PLIF system software (Insight 3G).

Separate tests were performed to verify that measurements were conducted within the linear fluorescence regime. When the illuminating spectral irradiance becomes too high within the measurement region, the emitted fluorescence can cross over from the linear regime to the saturated fluorescence regime (Eckbreth, 1996). The saturated fluorescence regime occurs when the lower energy state population of the fluorescing species is depleted due to excessive excitation to the elevated energy state. Although possible, quantification of the fluorescence signal within the saturated regime is more problematic, exhibiting reduced sensitivity and increased uncertainty due to the diminished response of the fluorescing species as a function of changes in concentration, and operating in the linear fluorescence regime is therefore generally preferred. The results of these tests demonstrated that experimental conditions were within the linear fluorescence regime, and a two-point calibration method was therefore implemented along with correction for background illumination and mean camera noise. The maximum concentration level (50 μg/L) resulted in sufficiently low molar absorption such that attenuation corrections were not required.

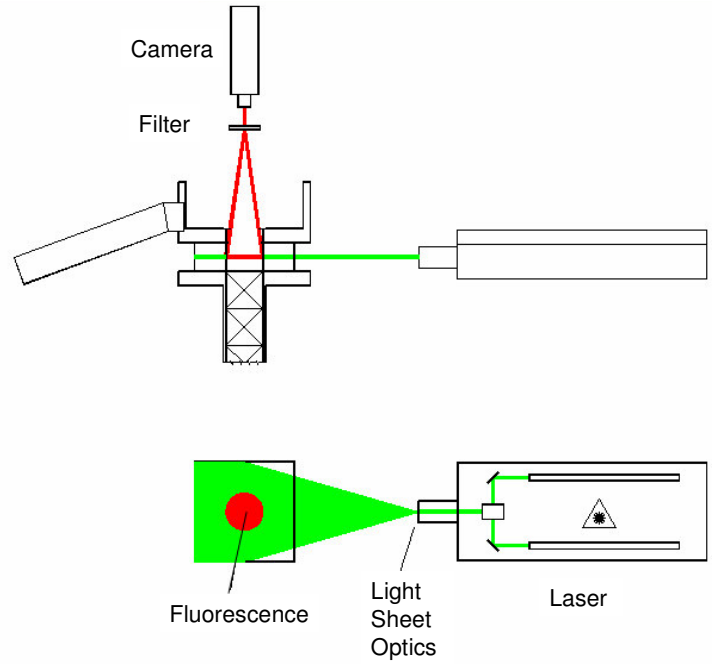

Fig. 2. Experimental layout, showing the vertically oriented camera, looking downward at a cross-section of vertically flowing fluid illuminated by the horizontal light sheet

The spatial resolution in PLIF measurements is generally limited by the thickness of the laser light sheet, rather than the pixel resolution of the camera as in other scientific imaging applications. This is because of the inherent averaging of the PLIF signal across the thickness of the laser light

that occurs during imaging (Crimaldi and Koseff 2001), and is especially true in turbulent mixing studies or IC engine research, since the mixing structures vary in size and are oriented (effectively) randomly in space. Structures that are smaller in scale that the light sheet thickness cannot generally be resolved since they will contribute only a portion of the light collected at a single pixel. This is the reason why PLIF imaging is often performed with pixel resolutions of 512 x 512 or lower. When larger imaging arrays are used, it is common to bin the image to match the effective pixel size to the (imaged) thickness of the laser light sheet, around 0.5 mm in general. In the case of the presented PLIF measurements of static mixing, however, the structures in the concentration field are not oriented randomly in space, but are rather organized in layers that are largely perpendicular to the laser light sheet. As such, the PLIF images presented have not been binned, maintaining the original 1376 x 1040 pixel resolution in the images. Structures at nearly half of the typically expected spatial resolution (400 μm) should be possible (Crimaldi and Koseff 2001).

3. PLIF Measurements

Concentration measurements were performed using a range of values for the (normalized) mixing length L/D, defined as the physical length, L, divided by the diameter of the pipe, D. In this case, the mixing length was increased by increasing the length of the SMX mixing unit. As the mixing length increases, the unmixed fluids are divided into an increasing number of layers with decreasing thickness. The combined effect of the increased residence time within the mixer and the smaller diffusion length scales associated with the finer layers leads to significant improvements in mixture homogeneity at the outlet. Mixing lengths of 4, 6, and 8 were examined. The measured concentration fields are shown in Figure 3. The scale values of the colorbars change among the three cases in order to highlight the concentration layering within the field at the different concentration levels. The thickness of the layers can clearly be seen to decrease from left to right, as the mixing length increases, although the overall geometric pattern remains similar as it is determined by the internal geometry of mixing elements.

A statistical analysis was performed to quantify the changes in the structure of the concentration field as the mixing length was varied. Figure 4 shows the location of the regions of interest that were used in this analysis. A rectangular region (dashed outline) was used to calculate the coefficient of variation, CoV (standard deviation divided by the mean concentration value), and to generate histograms of the enclosed concentration values, in order to provide a general characterization of the extent of mixing. Concentration profile graphs were calculated along the solid vertical line (Figure 4), in order to show the size of the fluid layers. The specific location of the profile location varied slightly among the three cases, in order to intersect nearby fluid layers at nearly perpendicular angles.

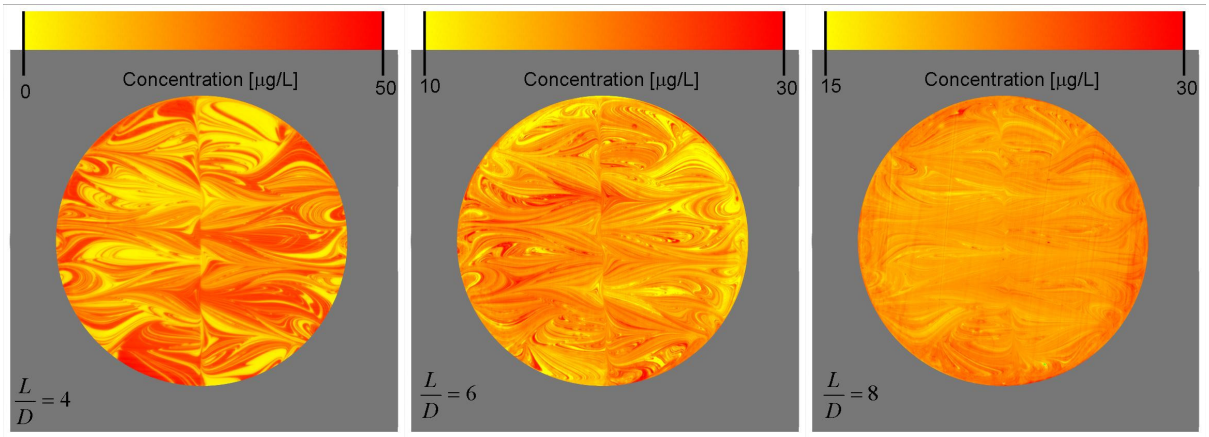

Fig. 3. Planar concentration maps for varying number of SMX static mixing units, or mixing length L/D. Increasing the mixing length subdivides the incoming fluid streams into an increased number of layers with decreasing thickness. Note the changes in intensity scaling between the three cases

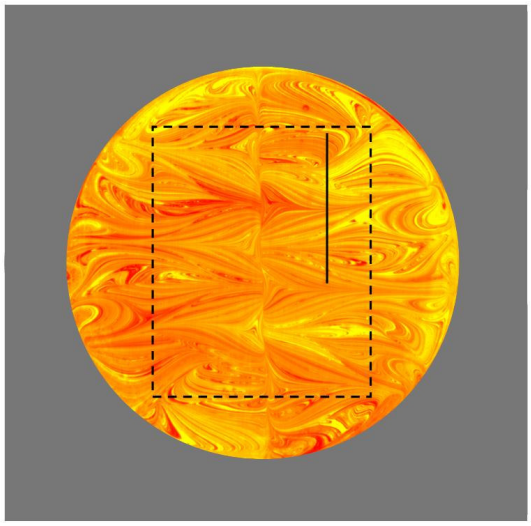

Fig. 4. Regions of interest used to examine concentration statistics of the results from Figure x. The concentration values within the dashed box were used for statistical analysis, and concentration profile graphs were calculated along the solid line

Figure 5 shows the concentration histograms and profile graphs for the three cases of mixing length, and Table 1 summarizes the statistics of the three cases. At the shortest mixing length, L/D = 4, the concentration histogram shows a largely unmixed field, with significant populations of concentration values at both very low (~ 5 μg/L) and high (~ 35 μg/L) concentration values. It has a mean value of about 21 μg/L and a mean value of 9.5 μg/L (CoV = 0.46). The associated profile graph shows fluid layers approximately 1 mm thick separating concentration changes as large as 30 μg/L.

Increasing the mixing length to L/D = 6 significantly improves the extent of mixing. The concentration histogram (Figure 5) changes from the relatively flat unmixed appearance to a more Gaussian-type distribution indicative of improved mixing, with a mean value of about 22 μg/L and standard deviation of 3.4 μg/L (CoV = 0.15). The concentration profile graph shows that the layer thickness has decreased, with significantly more layers between 0.5 mm and 1 mm in size. As the

mixing length increases to L/D = 8, the concentration histogram continues to grow narrower, with a mean value of 22 μg/L and standard deviation of 1.62 μg/L (CoV = 0.073). The thickness of the fluid layers, shown in the concentration profile, is now approaching several pixels in size at around 300 μm – 500 μm (the spatial scaling was approximately 57 μm/pixel).

L/D	Mean Concentration [μg/L]	Standard Deviation [μg/L]	CoV
4	20.7	9.46	.46
6	21.9	3.37	.15
8	22.3	1.62	.073

Table 1. Summary of statistics for the 3 cases of mixing length L/D

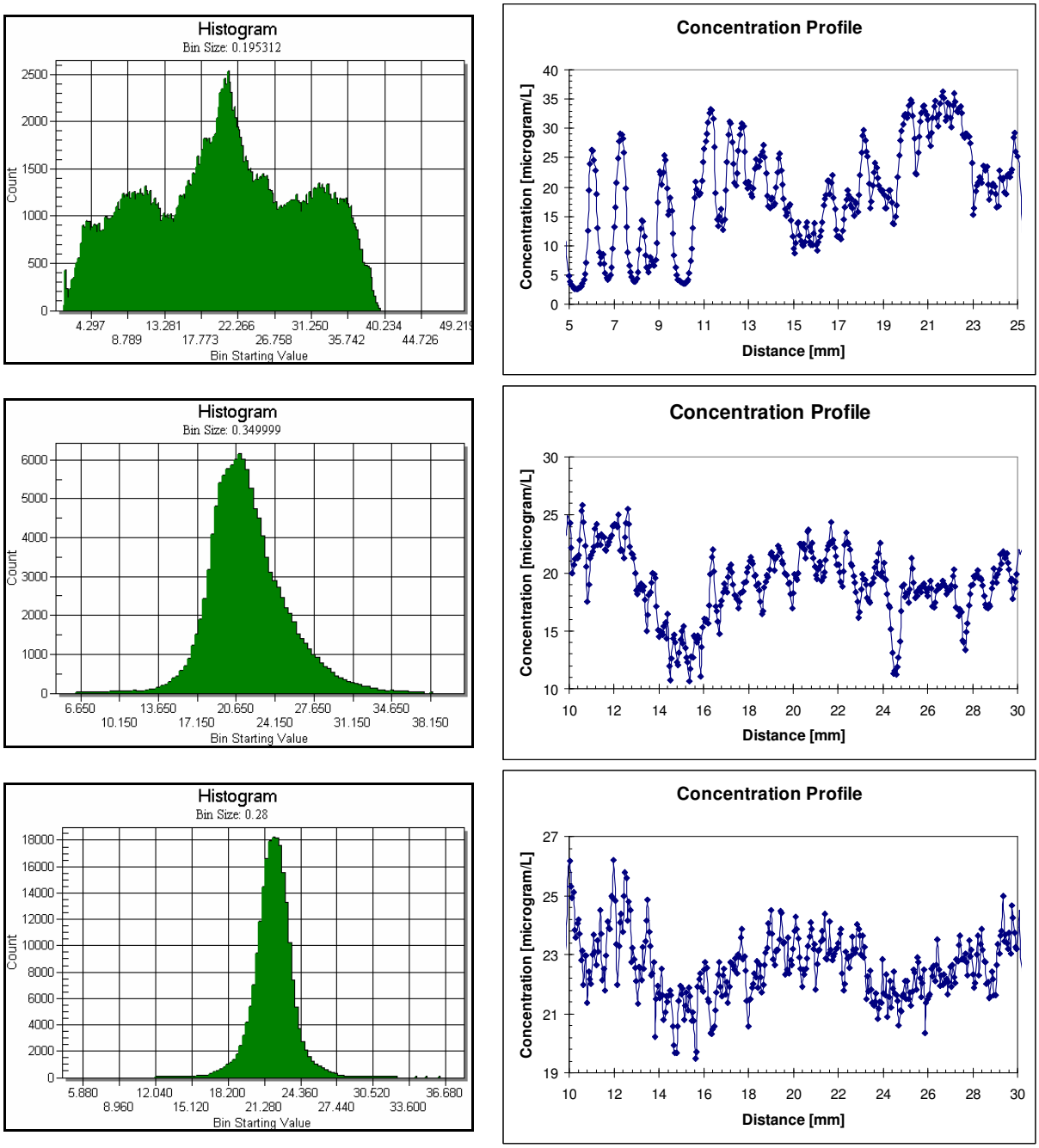

Fig. 5. Concentration histograms and profile graphs for the concentration fields: top row: L/D = 4, middle row: L/D = 6, bottom row: L/D = 8. Histograms were calculated from a large rectangular region (see Figure x) within the measurement region, and profile graphs were measured along a 20 mm vertical line in Figure x. The 20mm region is selected from a full profile graph to show the size of the fluid layers. The origin (x = 0) is the edge of the pipe

3. Conclusions

Planar laser-induced fluorescence (PLIF) measurements were used to quantify the spatial concentration distribution at the outlet of a laminar mixing device. The raw PLIF images were corrected for extraneous background signals and were processed using calibration images captured at uniform concentration values. Because the dominant structures in this flow were preferentially oriented parallel to the limiting dimension (perpendicular to the light sheet plane), the spatial resolution of the PLIF measurement was increased beyond the 400 μm thickness of the laser light sheet. Fluid layers as small as 200 μm to 300 μm were observed. The non-dimensional mixing length, L/D, was varied from 4 to 8, and changes in the concentration field were examined. The coefficient of variation decreased from 0.46 to 0.073 as the mixing length increased from 4 to 8, and the minimum thickness of the fluid layers decreased from above 1 mm to less than 400 μm.

References

Aguirre RC, Nathman JC, and Catrakis HC (2006) Flow Geometry Effects on the Turbulent Mixing Efficiency. Journal of Fluids Engineering 128, paper 027604JFG

Crimaldi JP, Koseff JR (2001) High-resolution measurements of the spatial and temporal scalar structure of a turbulent plume. Experiments in Fluids 31: 90 – 102

Eckbreth AC (1996) Laser Diagnostics for Combustion Temperature and Species. 2nd Ed. Gordon and Breach Publishers

Ghandhi JB (2006) Spatial resolution and noise considerations in determining scalar dissipation rate from passive scalar image data. Experiments in Fluids 40: 577 – 588

Hjertager LK, Hjertager BH, Deen NG, and T. Soldberg T (2003) Measurement of Turbulent Mixing in a Confined Wake Flow Using Combined PIV and PLIF. The Canadian Journal of Chemical Engineering 81

Kaiser SA and Long MB (2005) Quantitative planar laser-induced fluorescence of naphthalenes as fuel tracers. Proceedings of the Combustion Institute 30: 1555 – 1563

King GF, Lucht RP, and Dutton JC (1997) Quantitative dual-tracer planar laser-induced fluorescence measurements of molecular mixing. Optics Letters 22, No.9.

Probst DM, Strand TE, Rothamer DA, and Ghandhi JB (2001) The Effect of the Engine Flowfield on Spray Mixing in a DISI Engine. 14th Annual Conference on Liquid Atomization and Spray Systems

Ritchie BD and J.M. Seitzman JM (2001) Quantitative acetone PLIF in two-phase flows. AIAA paper 2001-0414

Ritchie BD, Mujumdar DR, and Seitzman JM, (2000) Mixing in Coaxial Jets Using Synthetic Jet Actuators. AIAA paper 2000-0404

Tian X, Roberts PJW (2003) A 3D LIF system for turbulent buoyant jet flows. Experiments in Fluids 35: 636 – 647

Tsurikoz MS and Clemens NT (2002) The structure of dissipative scales in axisymmetric turbulent gas-phase jets. AIAA paper 2002-0164

Xi C, Marks DL, Parikh DS, Raskin L, and Boppart SA (2004) Structural an functional imaging of 3D microfluidic mixers using optical coherence tomography. PNAS 101, No. 20: 7516 – 7521